

1 **Running head:** ???

2 Cranial morphological disparity within the  
3 adaptive radiation of tenrecs (Afrosoricida,  
4 Tenrecidae) is no greater than expected by  
5 chance

6 Sive Finlay<sup>1,2,\*</sup> and Natalie Cooper<sup>1,2</sup>

7 <sup>1</sup> School of Natural Sciences, Trinity College Dublin, Dublin 2, Ireland.

8 <sup>2</sup> Trinity Centre for Biodiversity Research, Trinity College Dublin, Dublin 2, Ireland.

9 \*sfinlay@tcd.ie; Zoology Building, Trinity College Dublin, Dublin 2, Ireland.

10 Fax: +353 1 6778094; Tel: +353 1 896 2571.

11 **Keywords:** disparity, morphology, geometric morphometrics, tenrecs,  
12 golden moles, adaptive radiation

## <sup>13</sup> **Abstract**

## 14 Introduction

15 Adaptive radiations, "evolutionary divergence of members of a single  
16 phylogenetic lineage into a variety of different adaptive forms" (Futuyma  
17 1998, cited by Losos, 2010) have long-attracted the interests and attentions  
18 of naturalists. Some of the most famous examples include cichlid fish and  
19 Caribbean *Anolis* lizards (Gavrillets & Losos, 2009). These groups exhibit  
20 great variety in both their phenotypic forms and the ecological niches  
21 which they occupy.

22 Each of these groups are uncontroversially accepted as examples of  
23 adaptive radiations. However, there has been considerable debate about  
24 how adaptive radiations should be defined (REFS) and how to distinguish  
25 an adaptively radiated group from just a clade of apparently diverse  
26 species. This is an important distinction because we need a consistent  
27 means of identifying an adaptive radiation before we can investigate and  
28 understand the selective pressures which cause adaptive radiations to  
29 develop in some groups and not others (REFS).

30 One suggestion is that an adaptively radiated clade should show  
31 exceptional (i.e. greater than expected by chance) morphological and  
32 ecological diversity (Losos & Mahler, 2010). In this case, a group of  
33 species would be considered exceptionally diverse if they have more  
34 phenotypic and ecological diversity than their closest relatives and also if  
35 they exhibit greater diversity than expected by chance. However, few  
36 putative examples of adaptive radiations have been characterised in this  
37 way. Under this definition it is equally important to demonstrate  
38 exceptional diversity in both phenotypic variety and the range of  
39 ecological niches which the species occupy. However, for the purposes of

40 this paper we will focus on the first criteria; investigating the evidence for  
41 morphological variety.

42 Phenotypic diversity is commonly measured as morphological  
43 disparity; the diversity of organic form (Foote, 1997; Erwin, 2007)). There  
44 is no single definition of disparity and it can be calculated in many ways  
45 including measures of morphospace occupation (e.g. Goswami et al., 2011;  
46 Brusatte et al., 2008) and rate-based approaches that assess the amount of  
47 directed change away from an ancestor (O'Meara et al., 2006; Price et al.,  
48 2013). Analyses of disparity apply these alternative approaches depending  
49 on whether the study is interested in current patterns of morphological  
50 diversity or the rate at which they accumulate through time.

51 Here we investigate current patterns of morphological disparity in  
52 tenrecs (Afrosoricida, Tenrecidae) to determine whether they represent an  
53 adaptive radiation sensu (Losos & Mahler, 2010). The tenrec family is  
54 comprised of 34 species, 31 of which are endemic to Madagascar (Olson,  
55 2013). From a single common ancestor (Asher & Hofreiter, 2006),  
56 Malagasy tenrecs diversified into a wide variety of descendant species  
57 which convergently resemble distantly related insectivore mammals such  
58 as shrews (*Microgale* tenrecs), moles (*Oryzorictes* tenrecs) and hedgehogs  
59 (*Echinops* and *Setifer* tenrecs) (Eisenberg & Gould, 1969).

60 Tenrecs are often cited as an example of an adaptively radiated family  
61 which exhibits exceptional morphological diversity (Soarimalala &  
62 Goodman, 2011; Olson & Goodman, 2003; Eisenberg & Gould, 1969).  
63 However, this apparent exceptional diversity is based on subjective  
64 comparisons to other groups and it has not been tested quantitatively. If  
65 tenrecs are exceptionally morphologically diverse then, following (Losos

66 & Mahler, 2010), tenrecs should be more morphologically disparate than  
67 expected by chance and they should exhibit significantly more phenotypic  
68 diversity than their nearest relatives, the golden moles (Afrosoricida,  
69 Chrysochloridae). Here we test these predictions using cranial  
70 morphology as a proxy for phenotypic diversity.

71 Using the most complete morphological data set of tenrecs and golden  
72 moles to date we apply geometric morphometric analyses (Rohlf &  
73 Marcus, 1993; Zelditch et al., 2012) to quantify morphological disparity  
74 among our species. Our results indicate that, on average, tenrecs are more  
75 phenotypically diverse than their closest relatives but their morphological  
76 diversity is no greater than that which is expected to evolve by chance.  
77 Therefore, under strict definitions, the designation of tenrecs as an  
78 exceptional adaptive radiation may need to be reconsidered.

79 These findings highlight the vital importance of testing our common,  
80 but often erroneous, expectations about patterns of morphological  
81 disparity in groups that exhibit apparent high levels of diversity.

## 82 **Materials and Methods**

### 83 **Data collection**

#### 84 **Morphological data collection**

85 One of us (SF) photographed cranial specimens of tenrecs and golden  
86 moles at the Natural History Museum London (NHML), the Smithsonian  
87 Institute Natural History Museum (SI), the American Museum of Natural  
88 History (AMNH), Harvard's Museum of Comparative Zoology (MCZ)

89 and the Field Museum of Natural History, Chicago (FMNH). We  
90 photographed the specimens with a Canon EOS 650D camera fitted with  
91 an EF 100mm f/2.8 Macro USM lens using a standardised procedure to  
92 minimise potential error (see supplementary material for details).

93 We collected pictures of the skulls in dorsal, ventral and lateral views  
94 (right side of the skull) and of the outer (buccal) side of the right  
95 mandibles. A full list of museum accession numbers and access to the  
96 images can be found in the supplementary material.

97 In total we collected pictures from 182 skulls in dorsal view (148  
98 tenrecs and 34 golden moles) and 181 mandibles in lateral view (147  
99 tenrecs and 34 golden moles), representing 31 species of tenrec (out of the  
100 total 34 in the family) and 12 species of golden moles (out of a total of 21  
101 in the family (Asher et al., 2010)). We used the taxonomy of Wilson and  
102 Reeder (2005) supplemented with more recent sources (IUCN, 2012;  
103 Olson, 2013) to identify our specimens.

104 We used a combination of both landmarks (type 2 and type 3,  
105 (Zelditch et al., 2012)) and semilandmarks to characterise the shapes of  
106 our specimens. Our landmarks (points) and semilandmarks (outline  
107 curves) used to represent shape variation in the dorsal skulls and  
108 mandibles are depicted in Figures 1 and 2 respectively. Corresponding  
109 landmark definitions for each view are in tables 1 and 2. We also placed  
110 landmarks and semilandmarks on photographs of ventral and lateral skull  
111 views, details can be found in the supplementary material. We digitised  
112 all landmarks and semilandmarks in tpsDIG, version 2.17 (Rohlf, 2013).

113 We re-sampled the outlines to the minimum number of evenly spaced  
114 points required to represent each outline accurately (MacLeod, 2013,

115 details in supplementary material). We used TPSUtil (Rohlf, 2012) to  
116 create sliders files (Zelditch et al., 2012) to define which points were  
117 semilandmarks. We conducted all subsequent analyses in R version 3.0.2  
118 (R Development Core Team, 2013) within the geomorph package (Adams  
119 et al., 2013). We used the gpagen function to run a general Procrustes  
120 alignment (Rohlf & Marcus, 1993) of the landmark coordinates while  
121 sliding the semilandmarks by minimising procrustes distance (Bookstein,  
122 1997). We used these Procrustes-aligned coordinates of all species (n=43)  
123 to calculate average shape values for each species which we then used for  
124 a principal components (PC) analysis with the plotTangentSpace function  
125 (Adams et al., 2013).

## 126 **Phylogeny**

127 Instead of basing our analyses on individual trees and assuming that their  
128 topologies were known without error (e.g. Ruta et al., 2013; Foth et al.,  
129 2012; Brusatte et al., 2008; Harmon et al., 2003) we used a distribution of  
130 101 pruned phylogenies derived from the randomly resolved mammalian  
131 supertrees in (Kuhn et al., 2011).

132 Eight species (six *Microgale* tenrecs and two golden moles) in our  
133 morphological data were not in the phylogenies. Phylogenetic  
134 relationships among the *Microgale* have not been resolved more recently  
135 than the (Kuhn et al., 2011) analysis, therefore we added the additional  
136 *Microgale* species at random to the *Microgale* genus within each phylogeny  
137 (Revell, 2012). We could not use the same approach to add the two  
138 missing golden mole species because they were the only representatives of  
139 their respective genera within our data. Therefore we randomly added

140 these species to the common ancestral node (using the findMRCA function  
141 in phytools (Revell, 2012)) of all golden moles within each phylogeny.  
142 Adding these extra species to the phylogenies created polytomies which  
143 we resolved arbitrarily using zero-length branches (Paradis et al., 2004).  
144 We calculated pairwise phylogenetic distances among species using the  
145 cophenetic function (R Development Core Team, 2013).

## 146 **Analyses**

### 147 **Disparity calculations**

148 We calculated morphological disparity separately for golden moles and  
149 tenrecs in each of the morphological datasets. We used the PC axes which  
150 accounted for 95% of the cumulative variation to calculate four disparity  
151 metrics; the sum and product of the range and variance of morphospace  
152 occupied by each family (Brusatte et al., 2008; Foth et al., 2012; Ruta et al.,  
153 2013). We also calculated morphological disparity directly from the  
154 Procrustes-superimposed shape data based on the inter-landmark  
155 distances among species pairs (ZelditchMD, Zelditch et al., 2012). We used

156 To test whether tenrecs have significantly different morphologies than  
157 golden moles, we used a non parametric MANOVA (Anderson, 2001) to  
158 compare morphospace occupation between the two groups and pairwise  
159 permutation tests to assess the evidence for significant differences in each  
160 disparity metric.

161 Sister taxon comparisons are inadequate on their own to determine  
162 whether a clade is exceptionally diverse (Losos & Miles, 2002). Therefore  
163 we repeated our morphometric analyses with a larger data set that



164 included other small mammal species to which tenrecs are considered to  
165 be convergent. We added specimens from hedgehogs (Erinaceidae, x  
166 specimens of x species), moles (Talpidae, x specimens of x species), shrews  
167 (Soricidae, x specimens of x species) and Solenodons (Solenodontidae, x  
168 specimens of 2 species).

## 169 **Results**

### 170 **Morphological disparity in tenrecs**

### 171 **Morphological disparity in tenrecs and golden moles**

172 Figures 3 and 4 depict the morphospace plots derived from our principal  
173 components analyses of average Procrustes-superimposed shape  
174 coordinates for each species in our skull and mandible data respectively.  
175 We used the principal components axes which accounted for 95% of the  
176 cumulative variation (n = 6 axes for the dorsal skulls analysis and n = 11  
177 axes for the mandibles) to calculate the disparity of each family.

178 In the dorsal skulls analysis, tenrecs and golden moles occupy  
179 significantly different areas of morphospace (npMANOVA,  $F = 59.34$ ,  $R^2 =$   
180  $0.59$ ,  $p = 0.001$ ) indicating that the two families have significantly different  
181 skull morphologies. For each of the calculated metrics, tenrecs have  
182 higher disparity than golden moles but these differences were not  
183 significant for the variance-based calculations. Non-*Microgale* tenrecs also  
184 higher disparity than golden moles but none of the comparisons were  
185 statistically significant .

186 Tenrecs and golden moles have significantly different mandible shapes

187 (npMANOVA  $F = 59.34$ ,  $R^2 = 0.59$ ,  $p = 0.001$ ). However, unexpectedly,  
188 golden moles appear to have higher disparity than tenrecs in the shape of  
189 their mandibles (although these differences are only significant when  
190 disparity is calculated as product of variance or ZelditchMD).

191 We tested whether these results may be artefacts of relatively low  
192 phenotypic diversity within *Microgale* tenrecs. However, although golden  
193 moles and non-*Microgale* tenrecs occupy significantly different areas of  
194 morphospace (npMANOVA  $F = 31.6$ ,  $R^2 = 0.59$ ,  $p = 0.001$ ), there is no  
195 significant difference between the two groups for any metrics of disparity.

## 196 Discussion

197 Our findings provide new insights into phenotypic diversity within the  
198 tenrec family and highlight the importance of testing assumptions about.  
199 Contrary to previous suggestions (e.g. Eisenberg & Gould, 1969; Olson,  
200 2013), tenrecs do not appear to be exceptional in their morphological  
201 diversity. Tenrecs are not more morphologically varied than expected to  
202 evolve by chance: they show significantly lower disparity in their  
203 morphologies than expected to evolve under Brownian Motion models of  
204 evolution.

205 When we compared tenrecs' cranial morphologies to their closest  
206 relatives the resulting patterns were less straightforward. For the analyses  
207 of skull shapes we found a trend towards higher disparity in tenrecs than  
208 in golden moles although these apparent differences were only significant  
209 for some disparity metrics. In contrast, the analyses of the mandibles  
210 indicated that golden moles have more diverse mandible shapes although,

211 again, these results are only significant for some disparity metrics.

212       These results put a new perspective on the long-standing assumption  
213 that tenrecs are an adaptive radiation.

214       It is evidence that tenrecs are a diverse group, both phenotypically and  
215 ecologically. Body sizes of extant tenrecs span three orders of magnitude  
216 (2.5 to >2,000g) which is a greater range than all other Families, and most  
217 Orders, of living mammals (Olson & Goodman, 2003). Within this vast  
218 size range there is striking morphological diversity, from the spiny  
219 *Echinops*, *Setifer* and striking *Hemicentetes* to the shrew-like *Microgale*.  
220 Furthermore, tenrecs inhabit a variety of ecological niches and habitats  
221 including terrestrial, arboreal, semi-aquatic and semi-fossorial forms  
222 (REFS). However, our results cast doubt over whether the evident  
223 diversity within the tenrec family should be considered to be a true  
224 adaptive radiation.

225       Phenotypic and ecological divergences within a clade are not  
226 surprising; most clades have at least small levels of disparity so, when it  
227 comes to identifying adaptive radiations, it's important to identify clades  
228 which are exceptional in their diversity (Losos & Mahler, 2010). Here we  
229 have presented the first quantitative investigation of morphological  
230 disparity in tenrecs and our results suggest that perhaps phenotypic  
231 variation in tenrecs is not the product of an adaptive radiation in the strict  
232 sense of its definition.

233       We found an overall pattern of higher disparity in tenrec skull shape  
234 than golden moles but only the range and Procrustes distance-based  
235 metrics are significant. This is probably because variance and range-based  
236 measures describe different aspects of morphospace occupation.

237 Another apparent anomaly in our results is that we found opposite  
238 patterns of group dissimilarities in the analyses of skulls and mandibles.  
239 The discrepancies could arise from factors associated with the modularity  
240 of morphological evolution.

241 There is strong evidence that morphological variation in skulls and  
242 mandibles is derived from differential evolution of integrated  
243 developmental modules (reviewed by Klingenberg, 2013). For example,  
244 there seems to be two primary modules in the mouse mandible; an  
245 alveolar part which holds the teeth and the ascending ramus for muscle  
246 attachment and which articulates with the skull (Klingenberg, 2008).  
247 Geometric shape covariation is stronger within rather than between these  
248 modules.

249 Our landmarks and curves for the mandibles (figure 2, table 2) include  
250 aspects of variation in the dentition but they focus particular attention on  
251 the ascending ramus (condyloid, condylar and angular processes).  
252 Therefore the higher morphological disparity in golden mole mandibles  
253 most likely reflects greater variation in the shape of the muscle attachment  
254 areas of the mandible. It proved impossible to position reliable landmarks  
255 on the corresponding mandibular articulation areas of the skull in lateral  
256 view (see supplementary). Therefore we could not test whether higher  
257 morphological disparity in the rami were correlated with associated  
258 morphological variety in the articulation areas of the skull.

259 If variation in muscle attachment/articulation sites is driving  
260 morphological disparity in mandibles, it is not clear why golden moles  
261 should have more disparate articular rami than tenrecs.

262 While our findings cast doubt on the designation of tenrecs as an

263 adaptive radiation sensu (Losos & Mahler, 2010), there are certain caveats  
264 to consider which could modify the interpretation of our results.

265 Phenotypic variation can evolve for reasons other than adaptive  
266 radiation. Therefore, to describe phenotypic divergence as the product of  
267 an adaptive radiations requires exceptional morphological diversity in  
268 traits which have specific and proven adaptive significance (Losos &  
269 Mahler, 2010). The evolution of cranial shape (both upper skull and  
270 mandible), particularly dental morphology, has obvious correlations with  
271 dietary specialisations (REFS) and occupation of specific ecological niches  
272 (REFS).

273 Considering the wide ecological diversity of our study species; the  
274 fossorial golden moles and semi-fossorial, arboreal, terrestrial and  
275 semi-aquatic tenrecs (REFS) it is reasonable to expect that this variety  
276 should be reflected in skull morphology. We assume that variation in  
277 cranial shape is an adaptive characteristic which allows the animals to  
278 survive in their divergent niches but we have not tested this assumption  
279 explicitly.

280 Cranial shape similarities are commonly used to delineate species  
281 boundaries (REFS) or for cross-taxonomic comparative studies of  
282 phenotypic (dis)similarities (REFS). However, disparity studies are  
283 inevitably constrained to be measures of diversity within specific traits  
284 rather than overall morphology (Roy & Foote, 1997). Therefore it is  
285 possible that other morphological proxies of phenotype; analyses of linear  
286 measurements and/or discrete characters of either cranial or post-cranial  
287 morphologies could yield different results.

288 However, the results of (Foth et al., 2012) are encouraging. In an

289 analysis of morphological disparity in pterosaurs, they found that  
290 disparity calculations based on geometric morphometric characterisation  
291 of skull shape yielded broadly similar results compared to analyses of  
292 whole-skeleton discrete characters and limb proportion data sets.  
293 Therefore the disparity patterns we find here based on geometric  
294 morphometric analyses of cranial shape most likely represent  
295 approximations of disparity which are accurate for morphological  
296 diversity in the clades.

297 These results highlight the importance of applying quantitative  
298 methods to testing our assumptions about adaptively radiated groups.

299 These analyses represent the first attempt to find evidence to support  
300 the common claim that tenrecs are an adaptive radiation. Future work  
301 will develop our results by expanding the analyses to non-cranial  
302 morphology and also measures of ecological diversity. However, our  
303 current results provide a clear indication that phenotypic variety within  
304 tenrecs is perhaps not as exceptional as it first seems and therefore their  
305 designation as an adaptive radiation may need to be re-considered.

## 306 **Acknowledgements**

307 We thank François Gould, Gary Bronner, Steve Brusatte, Steve Wang, Luke  
308 Harmon, Thomas Guillaume and the members of NERD club for  
309 insightful discussions and the museum staff and curators for their support  
310 and access to collections. Funding was provided by an Irish Research  
311 Council EMBARK Initiative Postgraduate Scholarship (SF) and the  
312 European Commission CORDIS Seventh Framework Programme (FP7)

313 Marie Curie CIG grant. Proposal number: 321696 (NC, SF)

## 314 **References**

- 315 Adams, D., Otárola-Castillo, E. & Paradis, E. 2013. geomorph: an r  
316 package for the collection and analysis of geometric morphometric  
317 shape data. *Methods in Ecology and Evolution* **4**: 393–399.  
318 10.1111/2041-210X.12035.
- 319 Anderson, M. 2001. A new method for non-parametric multivariate  
320 analysis of variance. *Austral Ecology* **26**: 32–46.  
321 10.1111/j.1442-9993.2001.01070.pp.x.
- 322 Asher, R. & Hofreiter, M. 2006. Tenrec phylogeny and the noninvasive  
323 extraction of nuclear DNA. *Systematic Biology* **55**: 181–194.
- 324 Asher, R.J., Maree, S., Bronner, G., Bennett, N., Bloomer, P., Czechowski,  
325 P., Meyer, M. & Hofreiter, M. 2010. A phylogenetic estimate for golden  
326 moles (Mammalia, Afrotheria, Chrysochloridae). *BMC Evolutionary*  
327 *Biology* **10**: 1–13.
- 328 Bookstein, F. 1997. Landmark methods for forms without landmarks:  
329 morphometrics of group differences in outline shape. *Medical image*  
330 *analysis* **1**: 225–243.
- 331 Brusatte, S., Benton, M., Ruta, M. & Lloyd, G. 2008. Superiority,  
332 competition and opportunism in the evolutionary radiation of  
333 dinosaurs. *Science* **321**: 1485–1488.
- 334 Eisenberg, J.F. & Gould, E. 1969. The Tenrecs: A Study in Mammalian  
335 Behaviour and Evolution. *Smithsonian Contributions to Zoology* **27**: 1–152.

- 336 Erwin, D. 2007. Disparity: morphological pattern and developmental  
337 context. *Palaeontology* **50**: 57–73.
- 338 Foote, M. 1997. The evolution of morphological diversity. *Annual Review of*  
339 *Ecology and Systematics* **28**: 129–152.
- 340 Foth, C., Brusatte, S. & Butler, R. 2012. Do different disparity proxies  
341 converge on a common signal? Insights from the cranial morphometrics  
342 and evolutionary history of *Pterosauria* (Diapsida: Archosauria). *Journal*  
343 *of Evolutionary Biology* **25**: 904–915. 10.1111/j.1420-9101.2012.02479.x.
- 344 Gavrillets, S. & Losos, J. 2009. Adaptive radiation: contrasting theory with  
345 data. *Science* **323**: 732–736. 10.1126/science.1157966.
- 346 Goswami, A., Milne, N. & Wroe, S. 2011. Biting through constraints:  
347 cranial morphology, disparity and convergence across living and fossil  
348 carnivorous mammals. *Proceedings of the Royal Society B: Biological*  
349 *Sciences* **278**: 1831–1839. 10.1098/rspb.2010.2031.
- 350 Harmon, L., Schulte, J., Larson, A. & Losos, J.B. 2003. Tempo and mode of  
351 evolutionary radiation in iguanian lizards. *Science* **301**: 961–964.
- 352 IUCN 2012. International Union for Conservation of Nature.
- 353 Klingenberg, C. 2008. Morphological integration and developmental  
354 modularity. *Annual review of ecology, evolution, and systematics* **39**:  
355 115–132.
- 356 Klingenberg, C. 2013. Cranial integration and modularity: insights into  
357 evolution and development from morphometric data. *Hystrix, the Italian*  
358 *Journal of Mammalogy* **24**: 43–58.



- 359 Kuhn, T., Mooers, A. & Thomas, G. 2011. A simple polytomy resolver for  
360 dated phylogenies. *Methods in Ecology and Evolution* **2**: 427–436.  
361 10.1111/j.2041-210X.2011.00103.x.
- 362 Losos, J. 2010. Adaptive radiation, ecological opportunity, and  
363 evolutionary determinism. American Society of Naturalists E. O. Wilson  
364 Award Address. *The American Naturalist* **175**: 623–639. 10.1086/652433.
- 365 Losos, J. & Miles, D. 2002. Testing the hypothesis that a clade has  
366 adaptively radiated: Iguanid lizards as a case study. *The American*  
367 *Naturalist* **160**: 147–157.
- 368 Losos, J.B. & Mahler, D. 2010. *Adaptive radiation: the interaction of ecological*  
369 *opportunity, adaptation and speciation*, chap. 15, pp. 381–420. Sinauer  
370 Association, Sunderland, MA.
- 371 MacLeod, N. 2013. Landmarks and semilandmarks: Difference without  
372 meaning and meaning without difference.
- 373 Olson, L. & Goodman, S. 2003. *Phylogeny and biogeography of tenrecs*, pp.  
374 1235–1242. The University of Chicago Press, Chicago.
- 375 Olson, L.E. 2013. Tenrecs. *Current Biology* **23**: R5–R8.
- 376 O'Meara, B., Ané, C., Sanderson, M. & Wainwright, P. 2006. Testing for  
377 different rates of continuous trait evolution using likelihood. *Evolution*  
378 **60**: 922–933. 10.1111/j.0014-3820.2006.tb01171.x.
- 379 Paradis, E., Claude, J. & Strimmer, K. 2004. Ape: Analyses of  
380 Phylogenetics and Evolution in R language. *Bioinformatics* **20**: 289–290.  
381 10.1093/bioinformatics/btg412.

- 382 Price, S., Tavera, J., Near, T. & Wainwright, P. 2013. Elevated rates of  
383 morphological and functional diversification in reef-dwelling haemulid  
384 fishes. *Evolution* **67**: 417–428. 10.1111/j.1558-5646.2012.01773.x.
- 385 Revell, L. 2012. phytools: an R package for phylogenetic comparative  
386 biology (and other things). *Methods in Ecology and Evolution* **3**: 217–223.
- 387 Rohlf, F. 2012. Tpsutil.
- 388 Rohlf, F. 2013. Tpsdig2 ver 2.17.
- 389 Rohlf, J. & Marcus, L. 1993. A revolution in morphometrics. *Trends in*  
390 *Ecology & Evolution* **8**: 129–132.
- 391 Roy, K. & Foote, M. 1997. Morphological approaches to measuring  
392 biodiversity. *Trends in Ecology & Evolution* **12**: 277–281.
- 393 Ruta, M., Angielczyk, K., Fröbisch, J. & Benton, M. 2013. Decoupling of  
394 morphological disparity and taxic diversity during the adaptive  
395 radiation of anomodont therapsids. *Proceedings of the Royal Society B:*  
396 *Biological Sciences* **280**: 20131071. 10.1098/rspb.2013.1071.
- 397 Soarimalala, V. & Goodman, S. 2011. *Les petits mammifères de Madagascar*.  
398 Guides sur la diversité biologique de Madagascar. Association Vahatra,  
399 Antananarivo, Madagascar.
- 400 Team, R.D.C. 2013. R: A language and environment for statistical  
401 computing.
- 402 Wilson, D. & Reeder, D. 2005. *Mammal species of the world. A taxonomic and*  
403 *geographic reference (3rd ed)*. Johns Hopkins University Press.

404 Zelditch, M., Swiderski, D. & Sheets, D. 2012. *Geometric Morphometrics for*  
405 *Biologists, second edition*. Academic Press, Elsevier, United States of  
406 America.

## 407 List of Figures

|     |   |   |    |
|-----|---|---|----|
| 408 | 1 | Landmarks (red points) and curves (blue lines) used to capture the morphological shape of skulls in dorsal view. Curves were re-sampled to the same number of evenly-spaced points. See table X for description of curves and landmarks.          |    |
| 409 |   | <i>Potamogale</i>   |    |
| 410 |   | <i>velox</i> (Tenrecidae) skull, accession number: AMNH_51327 . .   | 21 |
| 411 |   |   |    |
| 412 | 2 | Landmarks (red points) and curves (blue lines) used to capture the morphological shape of mandibles. Curves were re-sampled to the same number of evenly-spaced points. See table X for description of curves and landmarks.                      |    |
| 413 |   | <i>Potamogale</i>   |    |
| 414 |   | <i>velox</i> (Tenrecidae) mandible, accession number: AMNH_51327  | 22 |
| 415 |   |   |    |
| 416 | 3 | Principal components plot of the dorsal skulls' morphospace occupied by tenrecs (red, n=31) and golden moles (black, n=12). Axes are PC1 and PC2 of the average scores from a PCA analysis of mean Procrustes shape coordinates for each species. | 23 |
| 417 |   |   |    |
| 418 | 4 | Principal components plot of the mandibles' morphospace occupied by tenrecs (red, n=31) and golden moles (black, n=12). Axes are PC1 and PC2 of the average scores from a PCA analysis of mean Procrustes shape coordinates for each species.     |    |
| 419 |   |   |    |
| 420 |   |   |    |
| 421 |   |   |    |
| 422 |   |   |    |
| 423 |   |   |    |
| 424 |   |   |    |
| 425 |   |   |    |
| 426 |   |   |    |
| 427 |   |   |    |

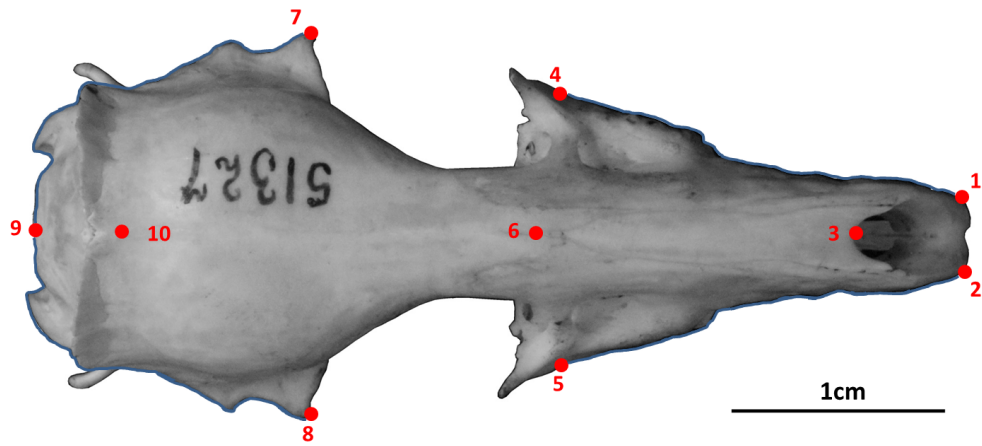


Figure 1: Landmarks (red points) and curves (blue lines) used to capture the morphological shape of skulls in dorsal view. Curves were re-sampled to the same number of evenly-spaced points. See table X for description of curves and landmarks. *Potamogale velox* (Tenrecidae) skull, accession number: AMNH\_51327

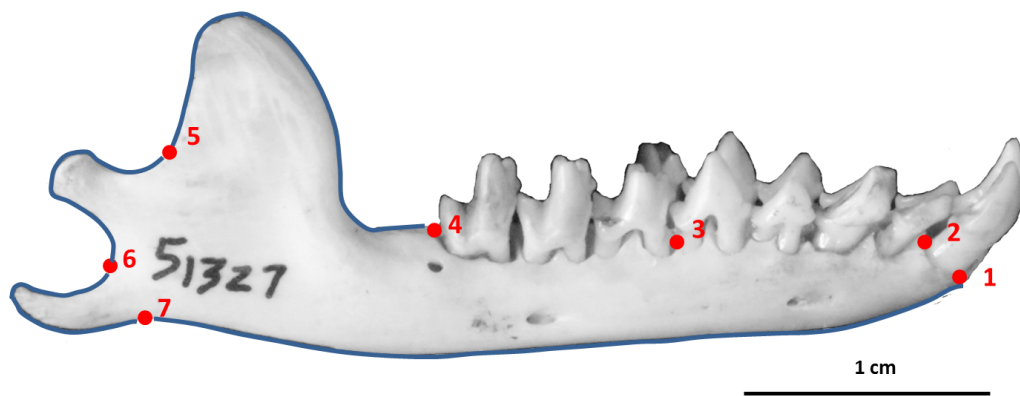


Figure 2: Landmarks (red points) and curves (blue lines) used to capture the morphological shape of mandibles. Curves were re-sampled to the same number of evenly-spaced points. See table X for description of curves and landmarks. *Potamogale velox* (Tenrecidae) mandible, accession number: AMNH\_51327

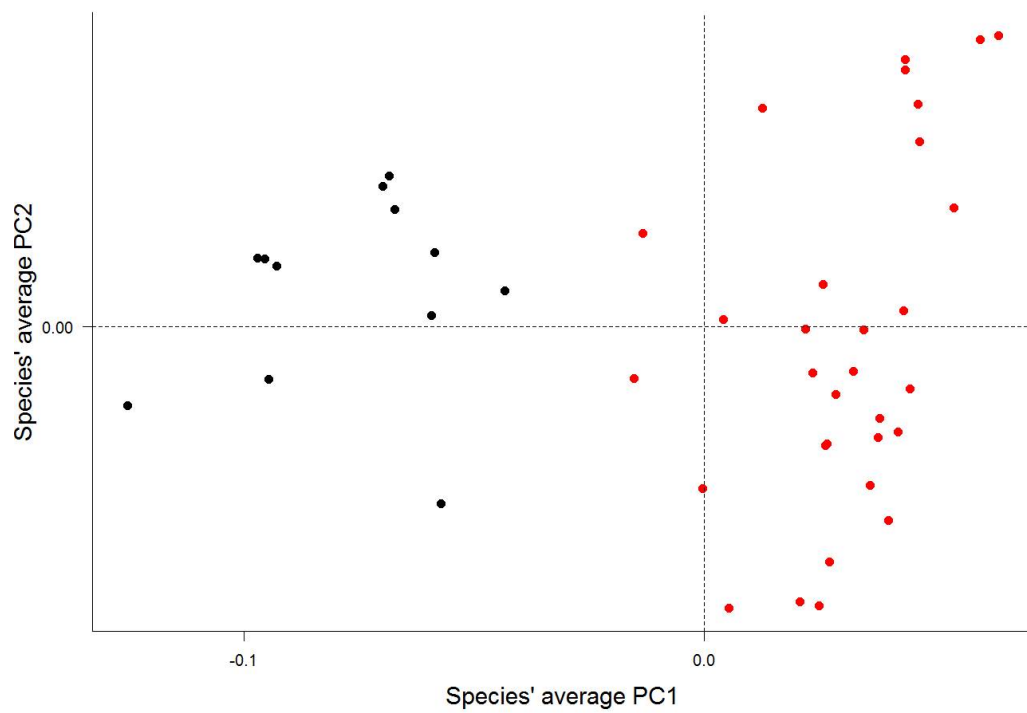


Figure 3: Principal components plot of the dorsal skulls' morphospace occupied by tenrecs (red,  $n=31$ ) and golden moles (black,  $n=12$ ). Axes are PC1 and PC2 of the average scores from a PCA analysis of mean Procrustes shape coordinates for each species.

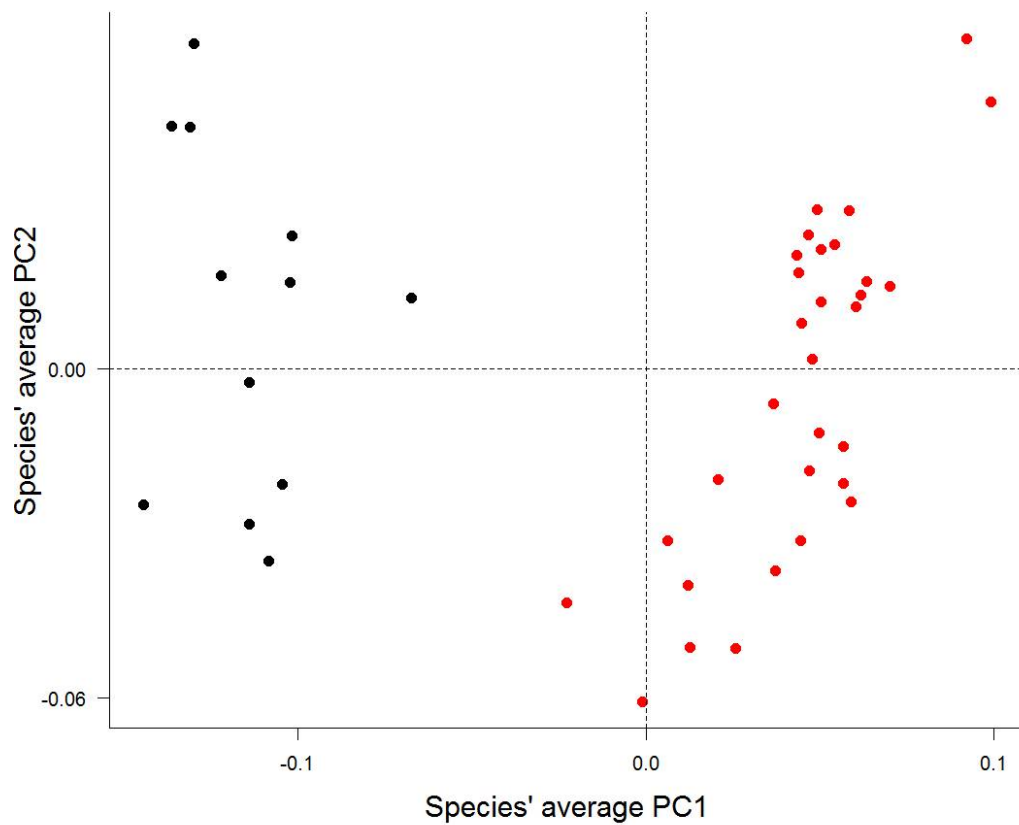


Figure 4: Principal components plot of the mandibles' morphospace occupied by tenrecs (red, n=31) and golden moles (black, n=12). Axes are PC1 and PC2 of the average scores from a PCA analysis of mean Procrustes shape coordinates for each species.



428 **List of Tables**

|     |   |  |    |
|-----|---|--|----|
| 429 | 1 | Descriptions of the landmarks (points) and curves (semi-         |    |
| 430 |   | landmarks) for the skulls in dorsal view (see Figure 1). . . . . | 26 |
| 431 | 2 | Descriptions of the landmarks (points) and curves (semi-         |    |
| 432 |   | landmarks) for the mandibles in lateral (buccal) view (see       |    |
| 433 |   | figure 2) . . . . .  | 27 |

Table 1: Descriptions of the landmarks (points) and curves (semilandmarks) for the skulls in dorsal view (see Figure 1).

| Landmark                      | Description   |
|-------------------------------|---|
| 1 + 2                         | Left (1) and right (2) anterior points of the premaxilla  |
| 3                             | Anterior of the nasal bones in the midline  |
| 4 + 5                         | Maximum width of the palate (maxillary) on the left (4) and right (5)   |
| 6                             | Midline intersection between nasal and frontal bones  |
| 7 + 8                         | Widest point of the skull on the left (7) and right (8)   |
| 9                             | Posterior of the skull in the midline   |
| 10                            | Posterior intersection between saggital and parietal sutures  |
| <b>Curve A</b><br>(12 points) | Outline of the braincase on the left side, between landmarks 9 and 7<br>(does not include visible features from the lower (ventral) side of the skull)  |
| <b>Curve B</b><br>(10 points) | Outline of the palate on the left side, between landamarks 4 and 1<br>(outline of the rostrum only, not the shape of the teeth)                         |
| <b>Curve C</b><br>(12 points) | Outline of the braincase on the right side, between landmarks 9 and 8<br>(does not include visible features from the lower (ventral) side of the skull) |
| <b>Curve D</b><br>(10 points) | Outline of the palate on the right side, between landamarks 5 and 2<br>(outline of the rostrum only, not the shape of the teeth)                        |

Table 2: Descriptions of the landmarks (points) and curves (semilandmarks) for the mandibles in lateral (buccal) view (see figure 2)

| Landmark | Description  |
|----------|--|
| 1        | Anterior of the alveolus of the first incisor                          |
| 2        | Posterior of the alveolus of the first incisor                         |
| 3        | Anterior of the alveolus of the first molar                            |
| 4        | Posterior of the alveolus of the last molar                            |
| 5        | Maximum curvature between the coronoid and condylar processes          |
| 6        | Maximum curvature between the condylar and angular processes           |
| 7        | Maximum curvature between the angular process and the horizontal ramus |
| Curve A  | Condylar process (between landmarks 4 and 5, 15 points)                |
| Curve B  | Condylar process (between landmarks 5 and 6, 15 points)                |
| Curve C  | Angular process (between landmarks 6 and 7, 15 points)                 |
| Curve D  | Base of the jaw (between landmarks 7 and 1, 12 points)                 |